Clays and Clay Minerals, Vol. 27, No. 3, pp. 161–174, 1979.

THERMAL TRANSFORMATION OF CHRYSOTILE STUDIED BY HIGH RESOLUTION ELECTRON MICROSCOPY

HELENA DE SOUZA SANTOS

Laboratório de Microscopia Eletrônica Instituto de Física
Universidade de São Paulo, São Paulo, Brazil

KEIJI YADA

Institute for Scientific Measurements, Tohoku University, Sendai, Japan

Abstract—Thermal transformation of chrysotile from Uruaçu District, state of Goiás, Brazil, heated in dry conditions at temperatures from 600°C to 1300°C was studied by high resolution electron microscopy and selected area electron diffraction (SAD). Up to 600°C, no morphological or SAD pattern changes were observed. At 600°C, the fibrils were still crystalline with the characteristics of the clinochrysotile. In addition, a new fringe system of 10–15 Å spacings appeared sporadically parallel to the 7.3 Å fringes of chrysotile. Areas of these extra fringes seem to constitute favorable sites for the nucleation of forsterite. At 650°C, forsterite nuclei appeared inside the nearly amorphous fibrils in the shape of patches consisting of flaky crystallites. At 700°C the chrysotile structure had disappeared; the new spots present in the SAD pattern were indexed as those of forsterite. Between 800–900°C the crystallinity of the patches was clearly demonstrated. From the lattice images in the patches, topotactic relations between chrysotile and forsterite were analyzed. At 1000°C very tiny grains of enstatite were formed mixed with forsterite grains. The SAD pattern is complex due to the coexistence of forsterite, enstatite, and silica-rich amorphous areas. From 1100°C to 1300°C the tridimensional growth of enstatite was promoted. The present results support the topotactic relations between chrysotile and forsterite found by X-ray analysis although differences up to several degrees may exist when these phases are observed microscopically. Evidence suggesting a topotactic growth between forsterite and enstatite was also obtained.

Key Words—Asbestos, Chrysotile, Electron Microscopy, Enstatite, Forsterite, Lattice-imaging, Selected Area Diffraction.

INTRODUCTION

Numerous publications describing the thermal transformation of the serpentine minerals indicate that when a fiber of chrysotile is heated in air forsterite is formed topotactically (Hey and Bannister, 1948; Brindley and Zussman, 1957; Glasser *et al.*, 1962); that is, a pseudomorph is formed that contains forsterite in one or more definite orientations with respect to the parent phase.

Differential thermal analysis (DTA), thermal gravimetric analysis (TGA), X-ray diffraction (XRD), and infrared spectroscopy (IR) have been used by many investigators (see Martinez, 1966) to study the thermal properties and structures formed during the transformations of serpentines. There is a broad, shallow endothermic reaction below 150°C during DTA due to the removal of surface water. The two principal reactions that characterize serpentine minerals, and in particular chrysotile, are represented by a large endothermic peak between 600°C and 720°C due to dehydroxylation, and an exothermic peak at 810°C caused by the formation of forsterite. The weight loss in TGA below 150°C is due to surface moisture, and the larger loss, about 14%, from 600°C to 750°C corresponds to the dehydroxylation endotherm noted in DTA.

Thermal-increment XRD indicates that chrysotile undergoes only minor changes below 500°C, but the dehydroxylation rate increases as the temperature is raised above 500°C. The loss of hydroxyls with the production of water vapor at about 600°C renders the mineral amorphous to X-ray diffraction (Ball and Taylor, 1963a). Above 700°C forsterite can be detected by XRD (Glasser *et al.*, 1962). At approximately 810°C a conversion of "chrysotile anhydride" takes place inside the fibrils which causes the exothermic peak noted in DTA, without destroying the fibrous appearance. Some of these previous studies have been made with chrysotile (Hey and Bannister, 1948), others with lizardite and massive serpentines (Brindley and Zussman, 1957; Brindley and Hayami, 1965).

The dehydration and recrystallization of serpentine proceeds in a crystallographically ordered manner. Considerable interest has been taken in possible mechanisms by which these topotactic relations are developed. This topotactic development of high temperature phases in platy lizardite was first interpreted in terms of a homogeneous process by Brindley and Zussman (1957) who wrote the overall reaction as:

$$\underset{\text{serpentine}}{2Mg_3Si_2O_5(OH)_4} \rightarrow \underset{\text{forsterite}}{3Mg_2SiO_4} + SiO_2 + 4H_2O$$

In this process, dehydration occurs uniformly throughout the crystal by the reaction of two hydroxyls as follows:

https://doi.org/10.1346/CCMN.1979.0270301 Published online by Cambridge University Press

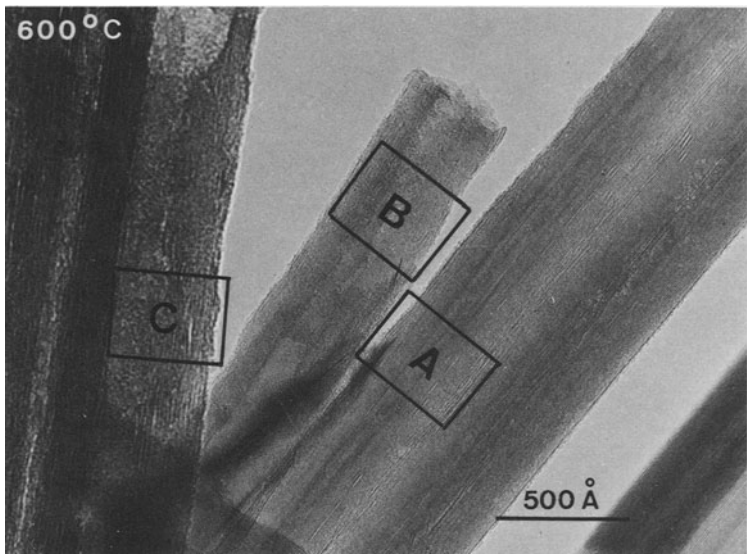

Figure 1. Electron micrograph of Uruaçu chrysotile fibrils heated at 600°C observed from a direction perpendicular to the fiber axis. The indicated areas are enlarged in Figure 2.

$$OH^- + OH^- \rightarrow H_2O\uparrow + O^{2-}$$

Although this process offered an explanation for the maintenance of the crystallographic order, it was difficult to explain the expulsion of water vapor and of silica at high temperatures without drastic changes in the crystal structure, while still preserving the external morphology of the crystal.

Ball and Taylor (1961, 1963a), Taylor (1962), and Brindley (1963a) suggested that more satisfactory explanations could be given in terms of heterogeneous processes. Ball and Taylor (1961) investigated the dehydration of brucite [$Mg(OH)_2$], and proposed a dehydration mechanism which they applied to the formation of forsterite from serpentine. They concluded that the dehydration and recrystallization are a combined type of reaction. Ball and Taylor (1963a) considered that the dehydroxylation and recrystallization of serpentine in air may proceed in four steps, as follows:

(1) Dehydroxylation—Donor and acceptor regions come into existence, and protons migrate to reaction zones where water molecules are liberated. Simultaneously, Mg and Si ions counter-migrate, and the oxygen packing remains essentially intact. This stage was represented by the authors as follows:

Acceptor regions: $7Mg_3Si_2O_9H_4 \rightarrow Mg_{27}Si_{18}O_{63}$

Donor regions: $2Mg_3Si_2O_9H_4 \rightarrow 18H_2O$

This means that after the loss of water from a region, it becomes porous, and the remaining oxygen accommodates all of the Mg and Si ions.

The "chrysotile anhydride" product is a partly disordered material giving an essentially "amorphous" X-ray powder diagram.

(2) Cation reorganization—Mg and Si ions begin to diffuse in opposite directions, forming Mg-rich and Si-rich regions.

(3) Forsterite formation—Mg-rich regions change to forsterite (Mg_2SiO_4), involving an ordering of the cations and changes in the oxygen packing. Stages (2) and (3) may be largely concurrent.

(4) Enstatite formation—At higher temperatures in dry heating, the Si-rich regions change to enstatite ($MgSiO_3$).

Brindley and Hayami (1965) confirmed the first stage of dehydroxylation and the formation of an X-ray amorphous phase, but proposed an alternate mechanism by which all or nearly all of the Mg ions, together with some of the Si ions liberated in the reaction zones where water is formed, migrate into the regions where forsterite is formed. The difficulty of forming enstatite in these regions is explained as arising from the sluggishness of the reaction of a more or less stable forsterite with excess silica. Inasmuch as the different morphological-structural forms of serpentine minerals give similar results, the thermal behavior is not dependent on the rolled layers of chrysotile or the planar layers of lizardite or massive serpentines.

Although the thermal transformation of serpentine minerals has been extensively studied, the visualization of the different stages (morphological changes inside the fibrils) has not been examined by electron-optical methods. The main objective of this present work is to study the chrysotile thermal transformations by high

https://doi.org/10.1346/CCMN.1979.0270301 Published online by Cambridge University Press

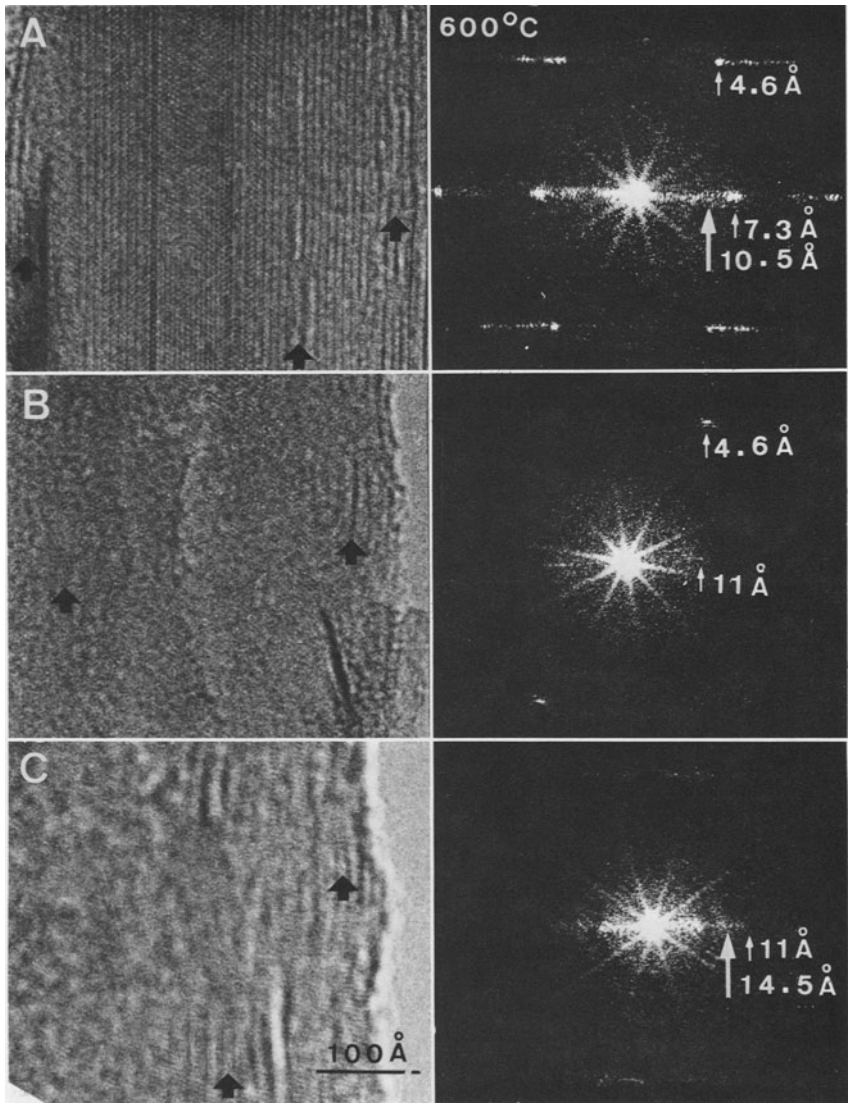

Figure 2. Enlarged areas shown in Figure 1: (A) shows a fibril whose structure is identical to unheated clinochrysotile. Three fringe systems corresponding to the spacings of 7.3 Å for (002), 4.5 Å for (020), and 4.6 Å for (110) are clearly visible. In addition, slightly distorted areas can be sporadically seen (arrows). (B) and (C) show respectively fringes of about 11 Å and 14 Å.

resolution, transmission electron microscopy and the crystallographic orientations of the products with respect to the parent crystal structure.

MATERIAL AND METHODS

A chrysotile asbestos specimen from Cana Brava mine, Uruaçu District, state of Goiás in Brazil (Souza Santos and Souza Santos, 1974) was used. It occurs as greenish white fiber veins, 1–2 cm long. A bundle of fibers was hand separated from the rock and tightly packed onto a platinum foil. It was heated dry in air in a temperature-controlled electric furnace at successively higher temperatures from 600°C to 1300°C (600°, 650°, 700°, 800°, 900°, 1000°, 1100°, 1200°, and 1300°C) for periods of 8 hr each. The samples were cooled naturally overnight. Fibers were hand picked from the heated chrysotile and placed on a perforated film (microgrid) reinforced with evaporated carbon. The fibers that spanned holes in the grids and that did not have substrate underneath were chosen for observation and photography.

A Siemens Elmiskop 101 electron microscope was used at 100 kV with a pointed filament. The microscope was modified to decrease both spherical and chromatic aberrations by employing the "pole piece-in-pole piece" system (Yada and Kawakatsu, 1976) and by in-

https://doi.org/10.1346/CCMN.1979.0270301 Published online by Cambridge University Press

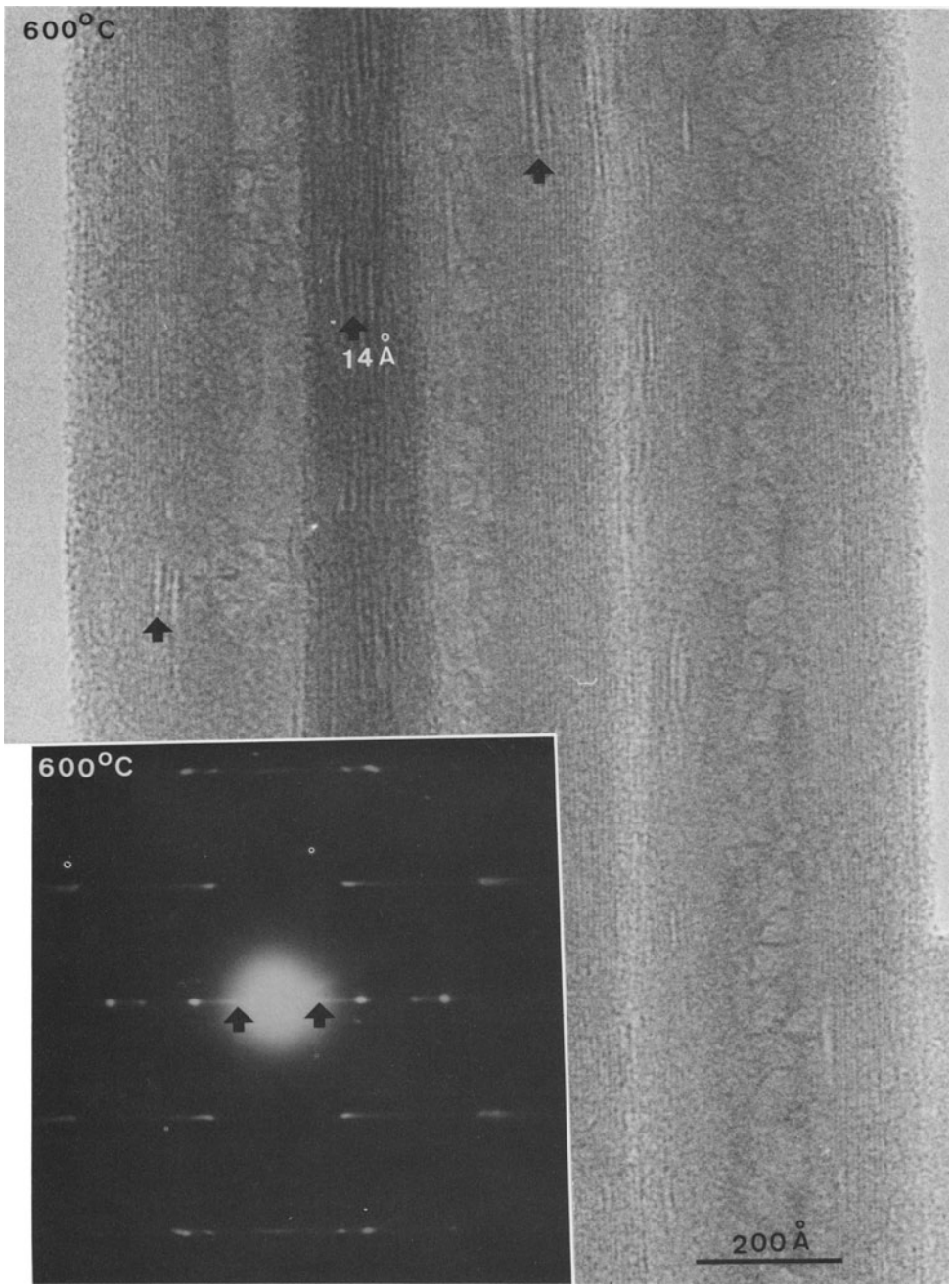

Figures 3 and 4. (3) SAD pattern from the fibril at 600°C, showing the new reflection corresponding to 14–15 Å spacing (arrows). (4) Coexistence of the original 7.3 Å fringes and 14 Å fringes sporadically distributed, without preferential localization in the fibril at 600°C (arrows).

creasing the excitation voltage of the objective lens. The direct electron optical magnification employed was 40,000 to 200,000 times.

RESULTS

After heat-treatment, the chrysotile fibers lost their flexibility and became harsh, changing color from gold to straw-yellow, but retained their asbestiform habit throughout the temperature range studied. The unheated Uruaçu fibrils yielded typical clinochrysotile selected-area electron diffraction patterns (SAD) (Yada, 1967, 1971). A histogram of the inner and outer diameters of the fibrils illustrates a remarkably wide distribution of diameters. None of the fibrils shows an

https://doi.org/10.1346/CCMN.1979.0270301 Published online by Cambridge University Press

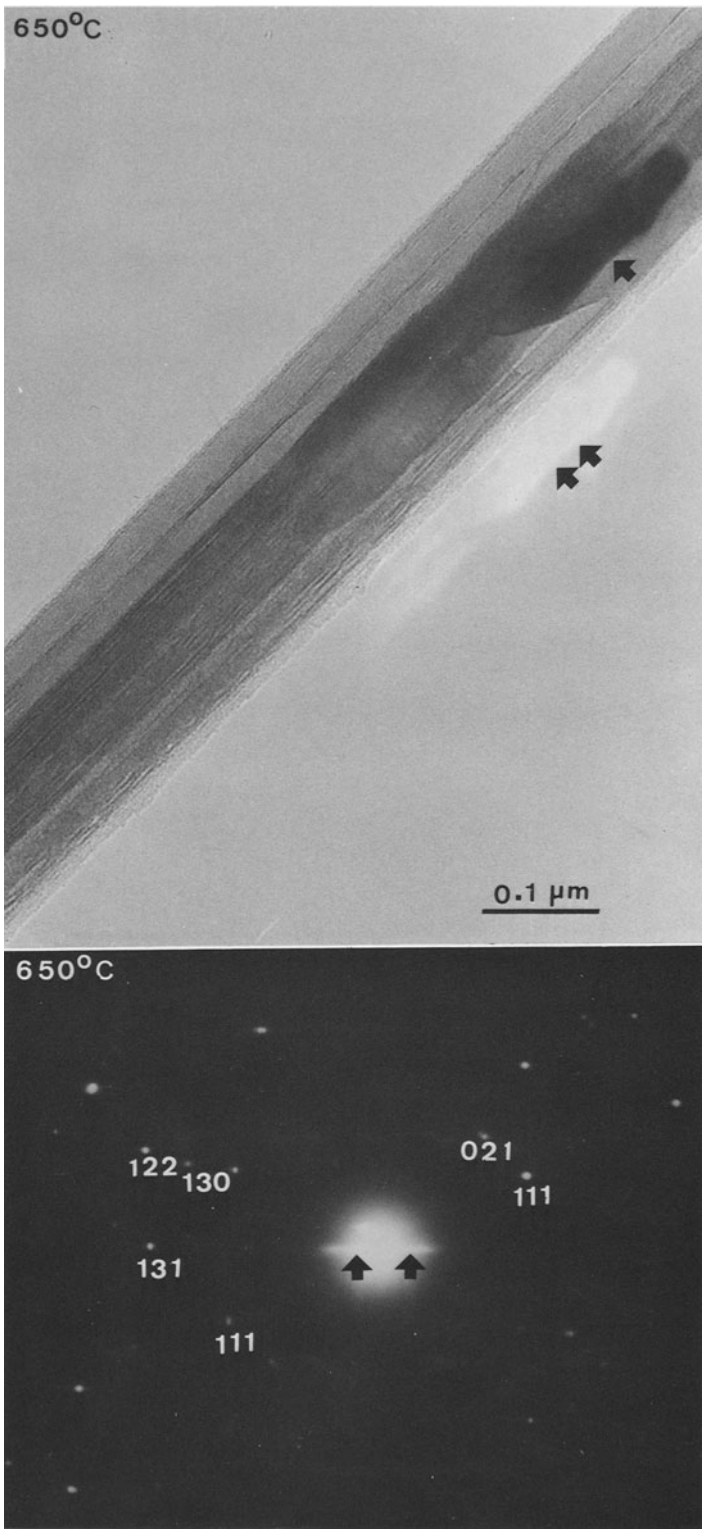

Figures 5 and 6. (5) Patch structures which start to appear at 650°C along the original fibril length. Bright-image on the background (double arrows) corresponds to a higher order reflection from the dark patch indicated by a single arrow. (6) At 650°C the SAD pattern includes many spots, together with a very unsharp clinochrysotile-like pattern. Many of the spots could be indexed on the basis of the structure of forsterite.

https://doi.org/10.1346/CCMN.1979.0270301 Published online by Cambridge University Press

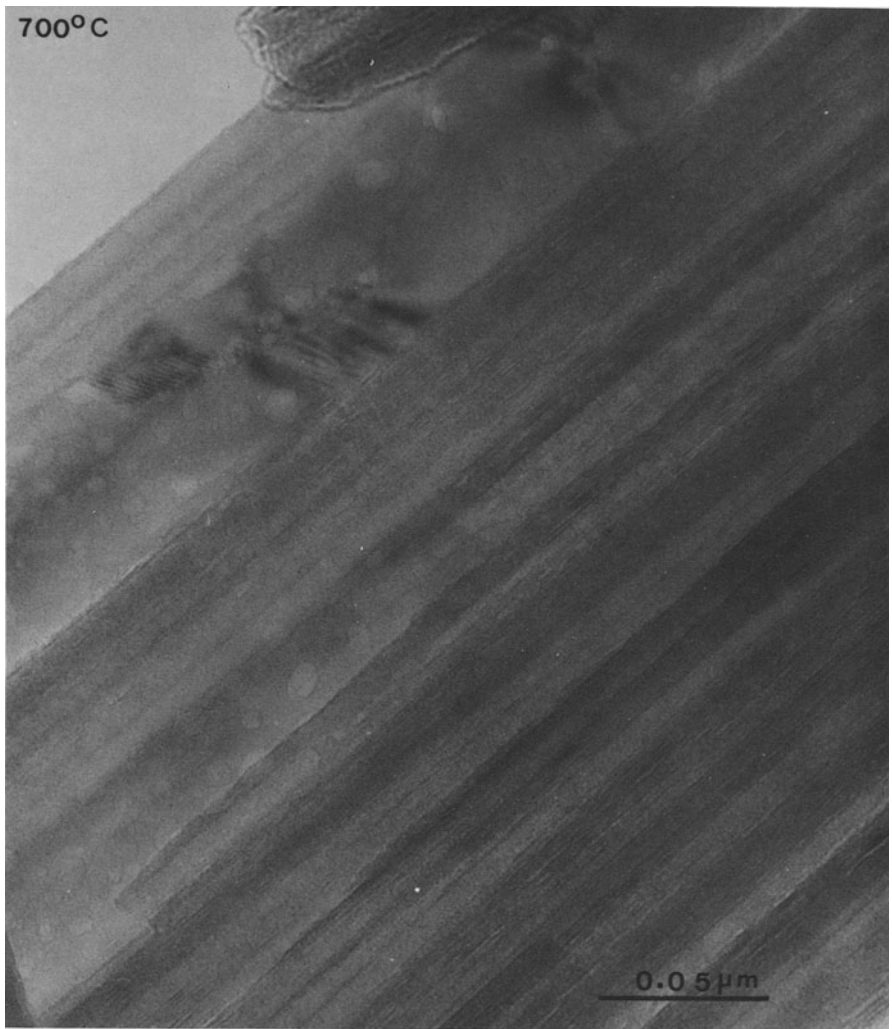

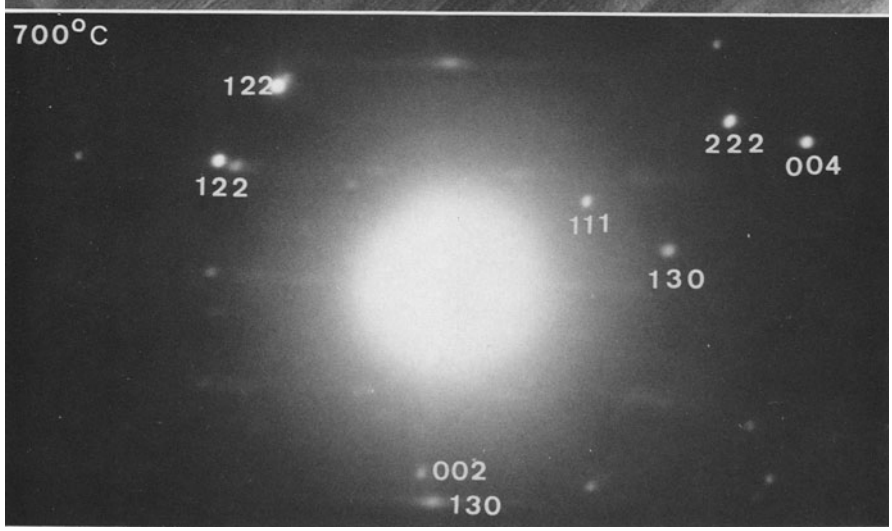

Figures 7 and 8. (7) Coalescence between fibrils has started at 700°C and in the coalesced areas, many voids, round and sometimes elongated, are included. (8) In the SAD pattern at 700°C the (00l) spots of chrysotile are almost absent, however, the 14–15 Å spots are visible together with other spots easily identified as being from forsterite.

https://doi.org/10.1346/CCMN.1979.0270301 Published online by Cambridge University Press

appreciable trace of a helical roll, and parachrysotile was rarely observed.

Below 600°C

At temperatures below 600°C the fibril and its SAD pattern are indistinguishable from those of the original unheated fibril.

600°C

At 600°C the fibrils are still crystalline, displaying morphologic and crystallographic characteristics of clinochrysotile. Special care was taken in observing the high resolution lattice at this stage, because the fibrils were still unstable under the electron beam. However, a new reflection, very broad and faint, appears on and along the zero layer line, corresponding to a 10–15 Å spacing. Figure 1 shows an electron micrograph of the chrysotile fibrils observed normal to the fiber axis. Areas A, B, and C are enlarged in Figure 2 with the corresponding optical diffraction patterns. Area A shows a fibril whose structure is identical to that of unheated clinochrysotile. Three fringe systems corresponding to spacings of 7.3 Å for (002), 4.5 Å for (020), and 4.6 Å for (110) are clearly visible. In addition, slightly distorted areas can be sporadically seen (arrows). Areas B and C show, respectively, fringes of about 11 Å and 14 Å. These fibrils are still crystalline, but approach an amorphous state, as shown by the optical diffraction patterns, where the original 7.3 Å fringes are almost absent. The degree of thermal reaction varies from fibril to fibril during this initial heating stage.

Figure 3 is an SAD pattern showing the new reflection corresponding to the 14–15 Å spacing. Figure 4 shows an example of the coexistence of the original 7.3 Å fringes and the 14 Å fringes sporadically distributed without preferential localization (arrows). The extent of this new fringe system is very limited (100–200 Å in length) and its spacing varies irregularly. Commonly observed values are 10–11 Å and 14–15 Å.

650°C

Although at 650°C no changes in the external morphology of the fibrils can be detected, irregularly shaped patch structures start to appear along the original fibril length. These patches, which appear to be very thin, are crystalline, because they commonly present Bragg reflections. In Figure 5, a bright image on the background (double arrow) corresponds to a higher order reflection from the dark patch indicated by a single arrow, which suggests that the dark patch is a flaky single crystal. At this stage, the 7.3 Å fringes are no longer clear in the lattice image; however, the new 14 Å fringes are abundant. In the SAD pattern, the 14–15 Å reflection is still present together with many new spots and a very unsharp clinochrysotile-like pattern in which (00l) reflections have nearly disappeared. With the aid of X-ray data, many of the new spots could be identified as due to forsterite (Figure 6).

700°C

At 700°C the external morphology of the fibrils is still present. The elongated patches cover much larger areas than before, but still are irregularly distributed along the length of the fiber bundle. Coalescence between fibrils has started, and in the coalesced areas, many voids, round or elongated, are present (Figure 7). In the lattice image, the 7.3 Å spacings are difficult to see in the fibril walls; however, the new 14 Å fringes are readily apparent (Figure 7). In the SAD pattern (00l) spots of chrysotile, such as (002), (004), and (006), are almost absent, while the 14–15 Å spot is clearly visible, together with other spots which can be easily identified as being from forsterite (Figure 8).

800°C

The external morphology of the fibril bundles remains at 800°C, but individual fibrils have coalesced to single thicker fibers in which many voids are present. The elongated patches have increased in length and diameter. accounting for a significant part of the fiber volume. The crystallinity of the patches is clearly demonstrated in dark field images. Figure 9 is an example of the lattice image in a patch showing three fringe systems of 3.85 Å, 5.1 Å, and 5.9 Å (2 × 2.99 Å), corresponding to the (021), (020), and (001) planes of forsterite, respectively. The 5.9 Å fringe system, which is perpendicular to the c-axis of forsterite, can be observed making a 67° angle with the oriented fiber length (as marked in Figure 9A). Figure 9B is the corresponding SAD pattern with sharp spots that can be indexed as reflections from forsterite with (011) orientations.

900°C

At 900°C the walls of the original fibril unit have lost their straight profile and have a scalloped appearence formed by the enlarged individual patches mentioned above (Figure 10A). Probably with the growth of forsterite grains, the patches have completely filled the original fibril, and the included voids have disappeared. Figure 12B shows the lattice image of the (020) planes of forsterite (5.12 Å fringe system) seen in the framed part of Figure 12A, almost perpendicular to the fibril length. This (020) fringe system suggests the relation $[010]_F$ // $[100]_C$. In the same micrograph of the same fibril, another finer fringe system can be seen on the original plate, corresponding to 4.3 Å and 2.99 Å spacings from (110) and (002) reflections. Thus, the SAD pattern can now be completely indexed and identified as that of forsterite.

https://doi.org/10.1346/CCMN.1979.0270301 Published online by Cambridge University Press

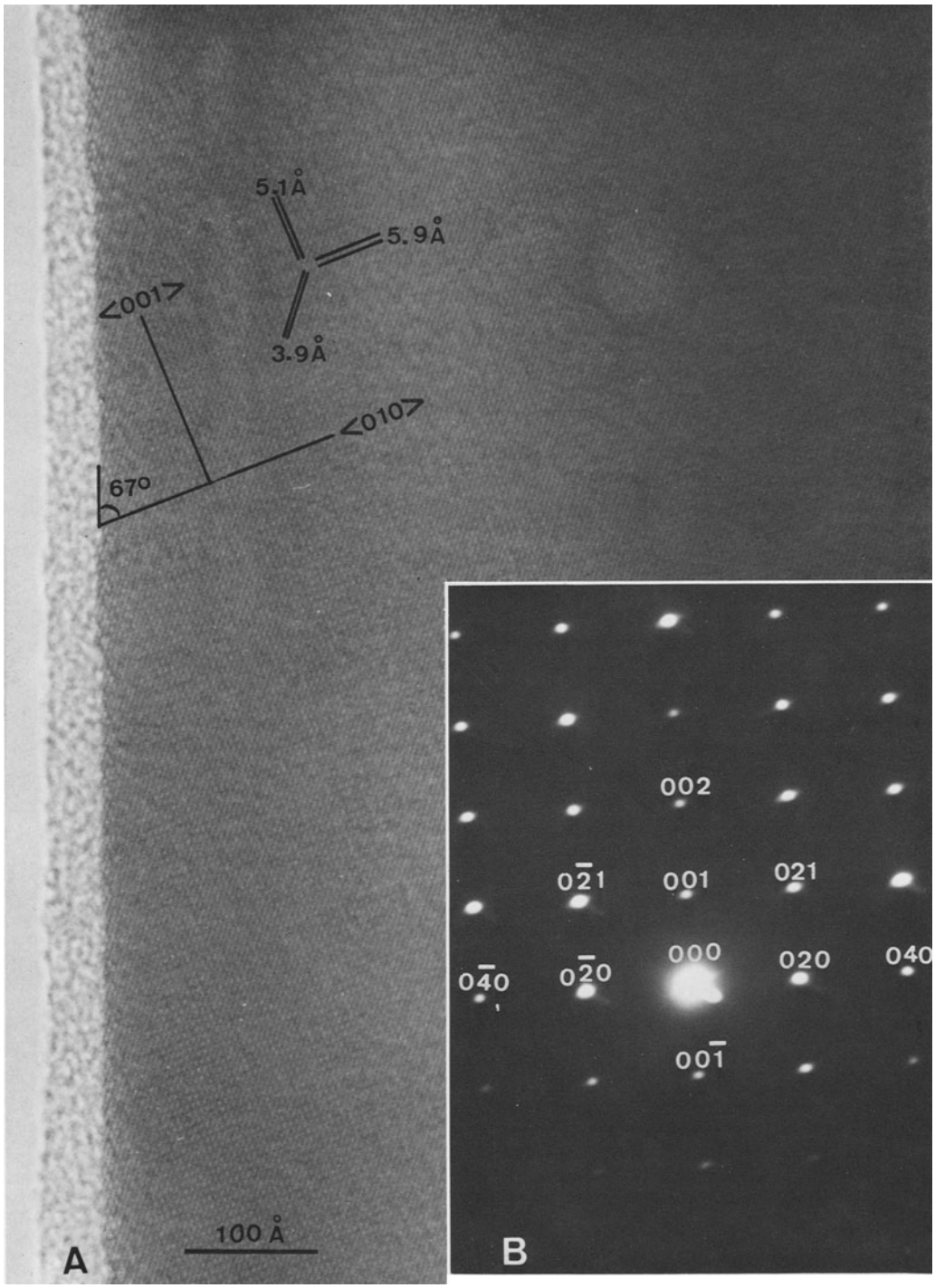

Figure 9. (A) Lattice image in a patch structure at 800°C, showing fringe systems of 3.9 Å, 5.1 Å, and 5.9 Å corresponding to the (021), (020), and (001) planes of forsterite, respectively. The 5.9 Å fringe system makes a 67° angle with the original fiber length. (B) corresponding SAD pattern whose sharp spots can be indexed being from forsterite at (011) orientation.

https://doi.org/10.1346/CCMN.1979.0270301 Published online by Cambridge University Press

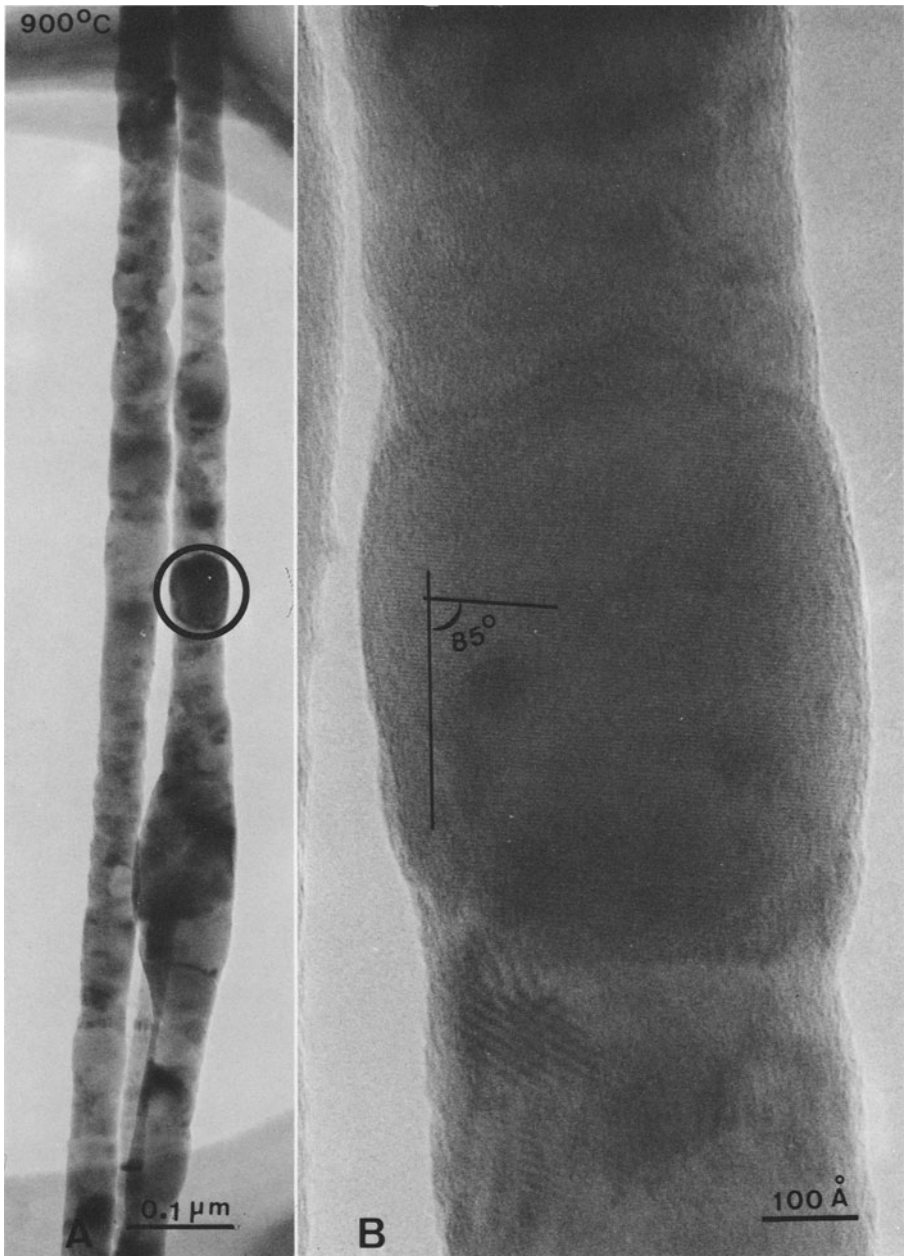

Figure 10. (A) At 900°C the walls of the original fibril unit present a scalloped appearence; wavy sites correspond to individual patch. The circled area is enlarged in (B), lattice image of (020) planes of forsterite (5.12 Å fringe systems) almost perpendicular (about 85°) to the fibril length.

1000°C

At 1000°C the fibrils are thicker in diameter due to tridimensional growth of the forsterite grains. The fibril bundles are commonly curved. Some grains in different orientations show contrast variation, depending on the Bragg condition. Also at this stage a new material, consisting of very tiny grains, has formed mixed with forsterite grains. At the lattice image level, fringe systems of 4.3 Å and 6.3 Å spacings corresponding to (020), (111), and (210) reflections from enstatite can be observed (Figure 11). The grain size of enstatite crystallites ranges from 100 Å to 400 Å. The SAD pattern consists of spots and rings and is complicated by the coexistence of forsterite, enstatite, and silica-rich areas (Figure 12). Most of the polycrystalline rings can be indexed as reflections from aggregates of orthorhombic

https://doi.org/10.1346/CCMN.1979.0270301 Published online by Cambridge University Press

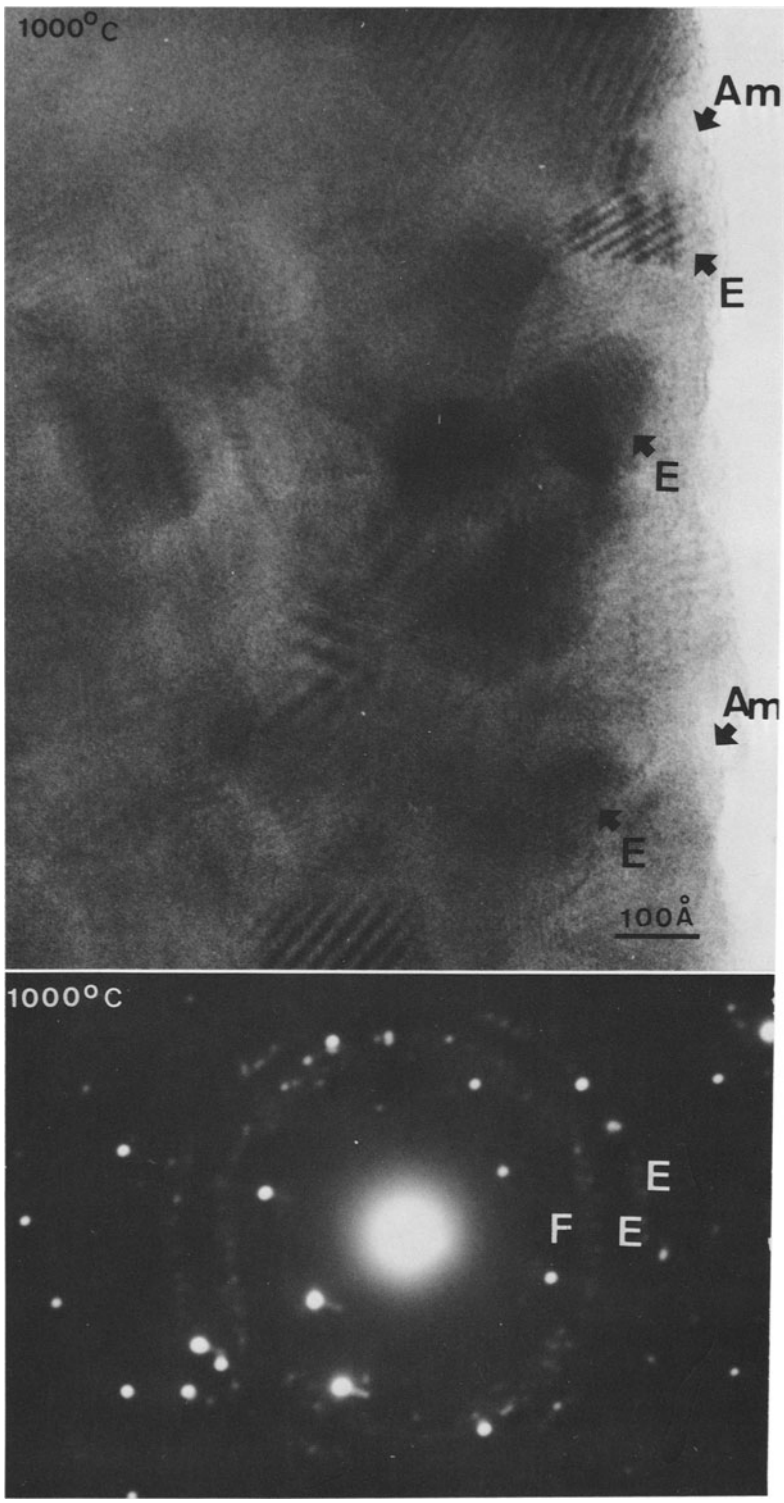

Figures 11 and 12. (11) At 1000°C the lattice image presents fringe systems corresponding to reflections from enstatite (E) as well as amorphous (Am) areas. (12) The SAD pattern is complicated at 1000°C by the coexistence of forsterite (F), enstatite (E), and silica-rich areas. Most of the polycrystalline rings can be indexed as being from enstatite crystallites, but they are slightly distorted from perfect circles.

https://doi.org/10.1346/CCMN.1979.0270301 Published online by Cambridge University Press

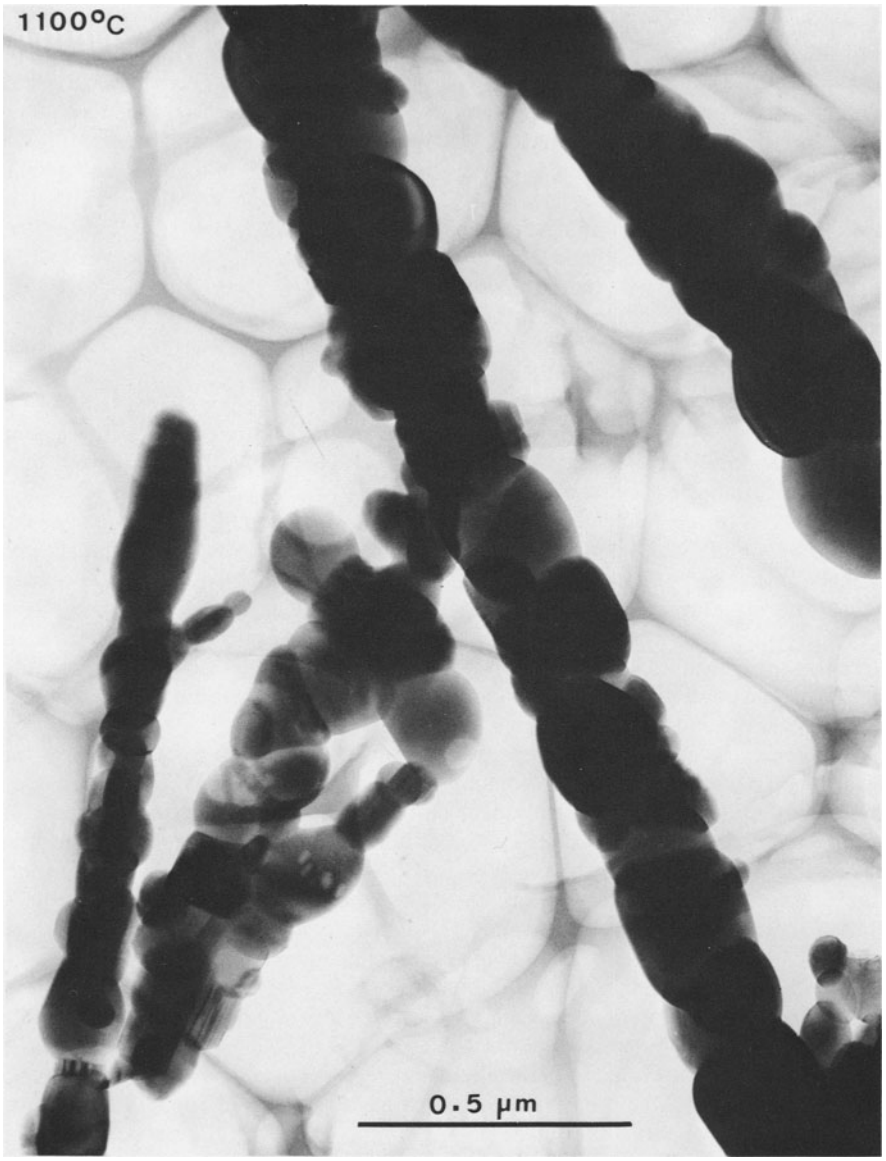

Figure 13. At 1100°C the original fibrils are completely changed into single twisted ropelike fibers, made up of a sequence of "knots."

enstatite crystallites. The slightly distorted circles are elongated in a direction perpendicular to the fibril axis, which suggests a preferentially oriented growth of enstatite crystallites with respect to the parent forsterite.

1000–1300°C

From 1100°C to 1300°C the original fibrils are completely changed into single twisted, ropelike fibers, consisting of a series of "knots" (Figure 13) produced by the tridimensional growth of the enstatite crystallites. Striated structures are common nearly parallel to the fibril length, reflecting the topotactic relation between forsterite and enstatite. At this stage the SAD patterns are complicated by tridimensional superposition of the crystallites and the striated structures in them, giving moiré spots and streaked spots, respectively. At 1300°C the tridimensional growth of enstatite is enhanced, and the SAD pattern can be more definitely indexed as due to enstatite. The grain size of enstatite reaches 1000–3000 Å at 1100°C and 3000–7000 Å at 1300°C.

DISCUSSION AND CONCLUSIONS

The extra spot observed in the SAD pattern at 600°C may correspond to what was described by Brindley and Zussman (1957) as a broad reflection, whose salient fea-

https://doi.org/10.1346/CCMN.1979.0270301 Published online by Cambridge University Press

tures are that it remain relatively stationary and fairly sharp at about 14–15 Å for the two-layer serpentine. The broadness of this new reflection is attributed to either the smallness of the corresponding areas or to local irregularity of the fringe spacing. Spacings at 14 Å were observed also in kaolin minerals fired at 700°C (Hill, 1965).

According to Brindley (1963b), the initial reaction (a nucleation process) may be one in which the OH-pair interaction occurs at favorable sites, with the formation of water molecules (*vide supra*). The nucleating surface is not necessarily an external surface but may be any defect which facilitates the initial reaction and permits escape of H_2O vapor at about 600°C. The extra fringes in the lattice image and the SAD spots of about 14 Å are probably caused by an intermediate structure produced by the dehydroxylation process and may represent favorable sites for forsterite nucleation. Defect areas of 10–11 Å fringes in Figure 2A seem to be a premonitory symptom of this phenomenon.

At 650°C the chrysotile structure could hardly be detected, either crystallographically (it was difficult to identify the 7.3 Å spots) or morphologically (the chrysotile lattice image was indistinct). The thin, elongated patch-areas inside the nearly amorphous fibrils may be interpreted as forsterite nuclei formed at the defective regions. Brindley (1963b) pointed out that it is difficult to decide whether the structural or the chemical aspect or both of the original minerals must be associated with this wide spacing, developed transitionally by the heat-treatment. In the present study, the correlation between the 14–15 Å SAD spacing and the lattice image of extra fringes of 11–14 Å, which exist transitionally between 600°C and 700°C (but which cannot be observed above 800°C), agrees with a chemical change giving rise to structural defects in the chrysotile fibril.

At 700°C chrysotile cannot be detected in either the lattice image or the SAD pattern; neither the 7.3 Å fringe system nor spots typical of chrysotile can be detected. The new spots in the SAD pattern can be indexed as due to forsterite. Thus, it can be concluded that at about 650°C forsterite forms two-dimensionally, that is, in the shape of very thin flakes, probably a few unit layers thick. At 700°C forsterite can be clearly identified.

Between 800°C and 900°C the forsterite areas start to define themselves as "inclusions" inside the fibrils suggesting that growth at this stage is fully tridimensional, completely modifying the fibril profiles and filling the fibril cores. Approximate dimensions of the forsterite grains at this stage are about 300–500 Å, depending on the original diameter of fibril bundle. Brindley and Hayami (1965) estimated the grain size of forsterite to be 400 Å as a lower limit from observed broadening of X-ray reflections, which agrees well with the present result. The forsterite SAD pattern is very sharp and suggests that structural distortion of the forsterite is minor as inferred by Brindley and Hayami (1965).

Brindley and Zussman (1957) concluded by X-ray analysis that forsterite is oriented with respect to the original serpentine mainly with $[010]_F \parallel [100]_S$ or $b_F \parallel a_S$; $[001]_F \parallel [010]_S$ or $c_F \parallel b_S$; and $[100]_F \parallel c_S^*$ or $a_F \parallel c_S$, though a relation $[001]_F \parallel [100]_S$ was sometimes weakly observed. Ball and Taylor (1963b) found two other orientations which are derived from the above prominent one by rotations of $\pm 60°$ about a_F.

The 5.12 Å fringe system corresponding to the (020) reflection of forsterite shows strong preferred orientation as seen in Figure 10B, where the direction of the fringe is nearly perpendicular (about 85°) to the original fibril length, that is $b_F \parallel a_C$. In this case the $(001)_F$ or $(002)_F$ reflection was not observed, but it can be said that the prominent topotactic relation is nearly satisfied. Another example which satisfied the relation more strictly within 3° was found, though omitted here. The fringe system of 5.9 Å (2 × 2.99 Å) corresponding to the (001) reflection of forsterite can be seen in Figure 9A making a 67° angle with the fibril length. Therefore, b_F makes an angle of 67° with respect to a_C. This corresponds to a rotation of the *bc* plane of forsterite by 60° about a_F.

Thus, the present results confirm that forsterite is formed in at least two orientations; the fiber direction of the chrysotile becomes either the *b* direction of forsterite, or a direction in the *bc* plane about 60° from the *b* direction of forsterite. However, it should be emphasized that the orientation relations found by X-ray analysis are not always held strictly, but should, when studied microscopically, have angular allowances up to several degrees.

The transformation of forsterite into enstatite starts at 1000°C and is complete at 1300°C; at 1300°C the forsterite crystals absorb silica and change to enstatite, giving the "knotted rope-like" regions in the micrographs. The enstatite lattice images are found at 1000°C; this agrees with Brindley and Hayami (1965), who reported that the retarded development of enstatite above 1000°C can be attributed to the sluggishness of the reaction of a more or less stable forsterite with excess silica.

In the models of both Ball and Taylor (1961) and Brindley and Hayami (1965) forsterite could coexist at 1000°C in the same fibril; this was readily apparent in the SAD pattern.

The following comments can be made about the SAD patterns from 600°C to 1300°C: (1) At 600°C, although there is an extra reflection with a broad peak at about 14 Å, corresponding to (001) of chrysotile, the clinochrysotile pattern is still very clear and sharp. (2) At 650°C the chrysotile pattern is faint but still present, and the extra reflection corresponding to 14 Å is sharper; also, some spots are present which could be indexed

as forsterite reflections. (3) At 700°C the chrysotile pattern becomes fainter, and the forsterite pattern is very sharp and can be fully indexed. (4) At 800°C and 900°C the forsterite pattern is perfectly clear. (5) At 1000°C a complex SAD pattern consisting of spots due to forsterite and rings due to enstatite crystallites, ranging from 100 Å to 400 Å, appears showing that forsterite and enstatite coexist with amorphous silica. It was ascertained that these rings cannot be due to crystalline silica. (6) At 1100°C the rings disappear and the SAD pattern becomes spotty because grains of enstatite have grown over the whole fibril. The spots are accompanied by streaks when the enstatite grains showing striated structure are due to stacking faults or microtwinning. At this stage forsterite is absent. Lamellae structure has often been observed parallel to the (100) of enstatite (Vander Sande and Kohlstedt, 1974; Iijima and Buseck, 1975). The lamellae structure seems to be similar to our striated structure in origin. Detailed analysis of this structure will be reported elsewhere, including the topotactic relation between forsterite and enstatite. (7) These observations hold up to 1200°C. (8) At 1300°C the enstatite SAD pattern becomes clear. This observation is in agreement with Ball and Taylor (1963a) who reported that the crystallization of forsterite is not a sudden process, but a gradual one, which begins with a small nucleus and spreads as the cation migration and packing changes proceed.

ACKNOWLEDGMENTS

This work was supported by a grant from "Conselho Nacional de Desenvolvimento Científico e Tecnológico," CNPq TC 2222.0431/75, to have Prof. Keiji Yada as a Visiting Professor at the University of São Paulo. Part of this paper was presented at the 6th International Clay Conference at Oxford, July 1978.

REFERENCES

Ball, M. C. and Taylor, H. F. W. (1961) The dehydration of brucite: *Mineral. Mag.* **32,** 754–765.

Ball, M. C. and Taylor, H. F. W. (1963a) The dehydration of chrysotile in air and under hydrothermal conditions: *Mineral. Mag.* **33,** 467–482.

Ball, M. C. and Taylor, H. F. W. (1963b) An X-ray study of some reactions of chrysotile: *J. Appl. Chem.* **13,** 145–150.

Brindley, G. W. (1963a) Crystallographic aspects of some decomposition and recrystallization reactions: *Prog. Ceram. Sci.* **3,** 3–55.

Brindley, G. W. (1963b) Role of crystal structure in solid state reactions of clays and related minerals: *Proc. Int. Clay Conf. 1963,* Stockholm **1,** 37–44.

Brindley, G. W. and Hayami, R. (1965) Mechanism of formation of forsterite and enstatite from serpentine: *Mineral. Mag.* **35,** 189–195.

Brindley, G. W. and Zussman, J. (1957) A structural study of the thermal transformation of serpentine minerals to forsterite: *Am. Mineral.* **42,** 461–474.

Glasser, L. S. D., Glasser, F. P., and Taylor, H. F. W. (1962) Topotactic reactions in inorganic oxy-compounds: *Q. Rev. Chem. Soc.* **16,** 343–360.

Hey, M. H. and Bannister, F. A. (1948) A note on the thermal decomposition of chrysotile: *Mineral. Mag.* **28,** 333–337.

Hill, R. D. (1965) 14 Å spacings in kaolin minerals: *Acta Crystallogr.* **8,** 120.

Iijima, S. and Busek, P. R. (1975) High resolution electron microscopy of enstatite. I: Twinning, polymorphism and polytypism: *Am. Mineral.* **60,** 758–770.

Martinez, E. (1966) Chrysotile asbestos: Relationship of the surface and thermal properties to the crystal structure: *Can. Min. Metall. Bull.* **69,** 414–420.

Souza Santos, H. and Souza Santos, P. (1974) The interaction of Reynolds lead citrate stain with chrysotile as observed by electron microscopy: *Proc. Second Latinamerican Congress on Electron Microscopy,* Brazil, 164–165.

Taylor, H. F. (1962) Homogeneous and inhomogeneous mechanism in the dehydroxylation of minerals: *Clay Miner. Bull.* **27,** 45–55.

Vander Sande, J. B. and Kohlstedt, D. L. (1974) A high resolution microscopy study of exsolution lamellae in enstatite: *Philos. Mag.* **29,** 1041–1049.

Yada, K. (1967) Study of chrysotile asbestos by a high resolution electron microscope: *Acta Crystallogr.* **23,** 704–707.

Yada, K. (1971) Study of microstructure of chrysotile asbestos by high resolution electron microscopy: *Acta Crystallogr.* **27,** 659–664.

Yada, K. and Kawakatsu, H. (1976) Magnetic objective lens with small bores: *J. Electronmicrosc.* (Japan) **25,** 1–9.

(Received 29 August 1978; accepted 17 December 1978)

Резюме—С помощью электронной микроскопии высокой разрешающей способности и электронной дифракции выбранной зоны (ДВЗ) изучалось термальное превращение хризотила из района Ураку, штат Гойас, Бразилия, нагреваемого в сухом виде до температур от 600°С до 1300°С. При нагревании до 600°С не наблюдалось ни морфологических изменений, ни измененний картины ДВЗ. При 600°С фибриллы оставались кристаллическими с характеристиками клинохризотила. Кроме того, появилась новая система полос с промежутками 10–15 Å, спорадически параллельная 7,3 Å полосам хризотила. Зоны этих дополнительных полос по-видимому являются благоприятными местами для образования центров кристаллизации форстерита. При 650°С центры кристаллизации форстерита появились внутри почти аморфных фибрил в форме включений, состоящих из чешуйчатых кристаллитов. При 700°С исчезла хризотиловая структура; новые пятна, появившиеся на картине ДВЗ были определены как пятна форстерита. Между 800°С и 900°С отчетливо была видна кристалличность этих пятен. По изображениям решеток в пятнах анализировались топотактические отношения между хризотилом и форстеритом. При 1000°С сформировались очень маленькие зерна энстатита, смешанные с зернами форстерита. Картина ДВЗ сложная из-за сосуществования форстерита, энстатита и богатых кремнеземом аморфных зон. От 1100°С до 1300°С происходил трехмерный рост энстатита. Полученные результаты подтверждают топотактические отношения между хризотилом и форстеритом, которые были обнаружены рентгеноструктурным анализом, хотя различия до нескольких градусов могут существовать, когда фазы наблюдаются под микроскопом. Получены также доказательства топотактических отношений между форстеритом и энстатитом при их развитии.

Resümee—Thermische Transformationen von Chrysotil vom Urauçu Distrikt, Staat von Goiás, Brasilien, erhitzt unter trockenen Bedingungen bei Temperaturen von 600°C bis 1300°C, wurde mittels Elektronenmikroskopie mit hohem Auflösungsvermögen und Elektronenbeugung ausgewählter Flächen (SAD) untersucht. Bis 600°C wurden keine Unterschiede in Morphologie oder SAD Bildern gesehen. Bei 600°C waren die Fäserchen immer noch kristallen mit den Eigenschaften des Klinochrysotil. Außerdem erschien sporadisch, parallel zu den 7,3 Å Rändern von Chrysotil, ein neues Randsystem mit Netzabständen von 10–15 Å. Die Flächen dieser extra Ränder scheinen günstige Plätze für die Kernbildung von Forsterit zu ergeben. Bei 650°C erschienen Forsteritkerne in den fast amorphen Fasern als Flecken, die aus schuppigen Kristallen bestehen. Bei 700°C war die Chrysotilstruktur verschwunden; die neuen Flecken in den SAD Bildern wurden als Forsterit katalogisiert. Zwischen 800–900°C wurde die Kristallinität der Flecken deutlich demonstriert. Aus den Gitterabbildungen in den Flecken wurden topotaktische Verwandtschaften zwischen Chrysotil und Forsterit analysiert. Bei 1000°C wurden sehr kleine Körner von Enstatit gemischt mit Forsteritkörnchen geformt. Das SAD Muster ist wegen der Koexistenz von Forsterit, Enstatit und silika-reichen, amorphen Flächen komplex. Von 1100°C bis 1300°C wurde das dreidimensionale Wachstum von Enstatit gefördert. Die vorliegenden Resultate unterstützen die topotaktischen Verwandtschaften zwischen Chrysotil und Forsterit, welche durch Röntgenanalyse gefunden wurden, obwohl etliche Grade Unterschiede existieren können, wenn die Phasen mikroskopisch untersucht werden. Beweise, welche ein topotaktisches Wachstum zwischen Forsterit und Enstatit vorschlagen, wurde auch erhalten.

Résumé—La transformation thermale de chrysotile du District d'Urauçu, état de Goiás, Brézil, chaufée sous des conditions sèches, de 600°C à 1300°C, a été étudiée par microscopie électronique à haute résolution et par diffraction électronique de régions sélectionnées (SAD). Aucun changement morphologique ou de clichés SAD n'a été observé jusqu'à 600°C. A 600°C, les fibrilles étaient encore cristallines avec les caractéristiques de clinochrysotile. De plus, un nouveau système de franges d'espacements 10–15 Å a apparu sporadiquement, parallèle aux franges 7,3 Å de chrysotile. Les régions de ces franges nouvelles semblent constituer des sites favorables pour la nucléation de forstérite. A 650°C, des nuclei de forstérite apparaissent à l'intérieur des fibrilles quasi amorphes en la forme de plaques constituées de cristallites floconneuses. A 700°C la structure de chrysotile avait disparu, les nouvelles tâches présentes dans le cliché SAD étaient classées comme étant celles de forstérite. Entre 800–900°C, la cristallinité des plaques était clairement démontrée. Des relations topotactiques entre la chrysotile et la forstérite ont été analysées à partir des images du réseau cristallin dans les plaques. A 1000°C, de très petits grains d'enstatite ont été formés, mélangés avec les grains de forstérite. Le cliché SAD est complexe à cause de la coexistence de forstérite, d'enstatite et de régions amorphes riches en silice. De 1100°C à 1300°C, la croissance en 3 dimensions d'enstatite a été promue. A présent, les résultats soutiennent les relations topotactiques entre la chrysotile et la forstérite trouvées par analyse aux rayons-X, quoique des différences jusqu'à plusieurs degrés peuvent exister lorsque les phases sont observées au microscope. Certaines preuves suggérant une croissance topotactique entre la forstérite et l'enstatite ont aussi été obtenues.